Industrial Crops & Products 223 (2025) 120050

Contents lists available at ScienceDirect

Industrial Crops & Products

journal homepage: www.elsevier.com/locate/indcrop

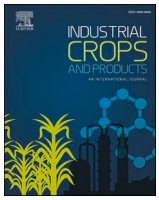

Transcriptome analysis reveals the impact of short-term biochar application on starch and sucrose metabolism in sweet potato tuberous roots

Jingzhen Zhang [a], Ximing Xu [a,b,*], Taojun Li [a], Zunfu Lv [a], Yueming Zhu [a], Jing Li [c], Guoquan Lu [a]

[a] The Key Laboratory for Quality Improvement of Agricultural Products of Zhejiang Province, Institute of Root and Tuber Crops, College of Advanced Agricultural Sciences, Zhejiang A&F University, Hangzhou 311300, China
[b] Key Laboratory of Biotechnology in Plant Protection of MARA and Zhejiang Province, Institute of Plant Virology, Ningbo University, Ningbo 315211, China
[c] Zhejiang Agricultural Technology Extension Center, Hangzhou 310020, China

ARTICLE INFO

Keywords:
Sweet potato
Short-term biochar application
Starch
Transcriptome sequencing

ABSTRACT

Biochar has been proven to be an effective method for enhancing sweet potato yield. However, limited research has been conducted on the molecular and physiological mechanisms underlying biochar's regulation of starch biosynthesis. This study aimed to investigate the transcriptome sequencing, which revealed the effects of short-term biochar application (STBA) on tuberous roots of sweet potato and the. We designed four STBA treatments: 0 t·hm^{-2} (CK), 5 t·hm^{-2} (X5t), 10 t·hm^{-2}(X10t), and 20 t·hm^{-2}(X20t), through a comprehensive analysis encompassing physiological data and RNA-seq analysis. The investigation included a comprehensive analysis integrating physiological measurements with RNA-seq data to elucidate the underlying mechanisms. The results showed that STBA enhanced the availability of nitrogen and potassium significantly, while also elevating the soil's pH levels. The 20 t·hm^{-2} STBA substantially enhanced sweet potato yields by 72.21 %, and the starch content of all STBA was not significantly different with CK. STBA decreased the sucrose, starch, glucose, and fructose content of tuberous root by 3–12 %, 1–5 %, 5–8 %, and 5–16 %. DEGs analysis identified distinct gene regulation patterns following biochar treatments, with the 5–10 t·hm^{-2} dosages predominantly down-regulating genes, including those in starch and sucrose metabolism pathways. WGCNA analysis uncovered 11 modules, highlighting biochar's influence on hormone signal transduction pathways, which was validated through qRT-PCR of five key genes. The study's findings light on the impact of STBA on the starch quality of sweet potatoes and inform biochar application strategies in agriculture.

1. Introduction

Agricultural organic waste (AOW) is a significant challenge for agriculture, with annual accumulations reaching nearly 3 billion tons (Alengebawy et al., 2023). Its smart recycling can stimulate soil fertility and decrease the need for chemical fertilizers, thus enhancing agricultural sustainability (Chen et al., 2020; Sayara et al., 2020). Addressing AOW effectively is now a key scientific pursuit. Biochar as a Bio-based material from crop materials has garnered significant attention as it provides a fantastic alternative for utilizing AOW (Tisserant and Cherubini, 2019). Biochar was produced from AOW under high-temperature, oxygen-limited conditions, and possesses a porous framework that alleviates soil compaction and optimizes nutrient and moisture retention, fostering robust crop development (Gabhane et al., 2020; Singh Yadav et al., 2023). Furthermore, its natural alkalinity (from straw sources) counters soil acidity, alleviates the adverse effects of aluminum and iron, and boosts phosphorus accessibility (Zhang et al., 2024).

Biochar studies are bifurcated into short-term (STBA) and long-term (LTBA) studies. STBA focuses on immediate soil and plant responses within a single season, examining biochar's rapid effects on soil fertility and plant development (Singh Yadav et al., 2023). Plants treated with 0.75 % STBA experienced less oxidative stress (Abideen et al., 2020). STBA significantly enhances the synthesis of stress-responsive proteins and proline in plants, thereby preserving their osmotic protection and potential under environmental stress (Haider et al., 2022). Starch is a key determinant of crops' quality. The effects of STBA on starch

* Corresponding author at: The Key Laboratory for Quality Improvement of Agricultural Products of Zhejiang Province, Institute of Root and Tuber Crops, College of Advanced Agricultural Sciences, Zhejiang A&F University, Hangzhou 311300, China.
E-mail address: xuximing@zafu.edu.cn (X. Xu).

https://doi.org/10.1016/j.indcrop.2024.120050
Received 19 September 2023; Received in revised form 6 November 2024; Accepted 10 November 2024
Available online 17 November 2024

properties and the activities of enzymes and expression levels of genes related to starch in two *Japonica* rice cultivars, and 5–10 t/hm^2 can regulate the activity of starch-related enzymes, and this affects the type, content, and fine structure of starch (Gong et al., 2020). STBA elevated the starch content and amylopectin ratio in broomcorn millet (Zhang et al., 2023), and increased the solubility, resistant starch, and swelling capacity in buckwheat, but decreased the amylopectin (Tao et al., 2023). Hence, starch properties across various crops display diverse responses to STBA.

Sweet potato *(Ipomoea batatas* L.) is an industrial crop with high starch content (50–80 % on a dry weight basis), starch extraction rate and its quality are pivotal in assessing the suitability of sweet potatoes for use in the starch industry and as a source for bioenergy production (Lyu et al., 2021). The positive influence of biochar on the levels of key nutrients such as nitrogen, phosphorus, potassium, calcium, magnesium, and sulfur, which are vital for the growth and quality of sweet potatoes (Agbede et al., 2024; Singh et al., 2022; Walter and Rao, 2015). However, the direct effect of biochar on the enzymes and pathways involved in starch synthesis has not been extensively studied. Understanding these effects could provide insights into how biochar application might be optimized to improve the yield and quality of sweet potato starch, which is a significant component of the crop's economic and nutritional value (Lai et al., 2016). The impact of biochar on starch synthesis in sweet potatoes is a topic that warrants further investigation. While it is known that biochar can improve soil health and potentially enhance crop yields and quality by affecting various soil properties, the specific influence on the starch synthesis process in sweet potatoes remains less explored. Further investigation is warranted to clarify the mechanisms of biochar's interaction with soil and plant systems concerning starch synthesis.

Consequently, in this study, we applied four STBA treatments: 0 t·hm^{-2} (CK), 5 t·hm^{-2} (X5t), 10 t·hm^{-2} (X10t), and 20 t·hm^{-2}(X20t), through a comprehensive analysis encompassing physiological data and RNA-seq analysis, which aimed to improve both the yield and quality of sweet potato by applying different biochar to soil and analyzing transcriptional modification in tuberous roots. We hope this research could provide a novel insight that deepens our comprehension of biochar's influence on crops and also furnishes a theoretical foundation and practical guidance for achieving high-yield sweet potato cultivation in reclaimed land and extending biochar applications to other crops.

2. Materials and methods

2.1. Plant materials and growth environment

The pot experiment was conducted from April to October across the years 2022 and 2023 at the farm of Zhejiang A & F University, Hangzhou, Zhejiang Province, China (30°15′N, 119°43′E). The sweet potato cultivar tested was Xinxiang, a high-quality conventional sweet potato cultivar. The soil bulk density is 1.35 g/cm^3, and soil quality was calculated for the top 20 cm layer. The biochar was produced and supplied by Liaoning Golden Future Agricultural Development Co., Ltd. China. The experimental treatments comprised four STBA treatments: 0 t·hm^{-2} (CK), 5 t·hm^{-2} (X5t), 10 t·hm^{-2}(X10t) and 20 t·hm^{-2}(X20t). The amount of biochar was calculated according to Gong et al. (2009). The biochar was mixed with soil into the pots 2 days before sweet potato transplanting. Plastic buckets with a diameter of 40 cm and height of 30 cm were filled with 8 kg of dry soil and then mixed with biochar, with 30 pots per treatment, and two holes for planting sweet potatoes in each pot. The experimental setup incorporated a precise drip irrigation system, featuring a specifically chosen drip tape with a radius of 10 millimeters, and drip emitters delivering a flow rate of 3.0 liters per hour at intervals of 0.3 m. Following the planting of sweet potato slips, an initial irrigation of 100 liters per pot was administered for three days to establish the crop. Subsequently, a reduced watering regimen of 50 liters per pot was maintained and applied every two days. Samples of the tuberous roots, leaves, and stems were meticulously collected in triplicate for each treatment and site 130 days after planting, employing a randomized selection process to ensure representativeness and minimize bias in the data.

2.2. Soil nutrients properties

The biochar specimens were procured in advance of the experimental procedures, whereas the soil samples from the various treatments were gathered after the sweet potato harvest, providing a post-experimental analysis of soil conditions. The soil's nutritional properties, encompassing carbon, available nitrogen, available phosphorus, and available potassium content, were precisely determined using an elemental analyzer (Vario EL cube, Elementar, Germany) across the spectrum of experimental treatments. (Ye et al., 2020). The pH values of the biochar, soil, and treatment samples were analyzed using a pH/ion meter (SDT-60, Zhejiang Top Cloud Agriculture Technology Co., Ltd).

2.3. Dry matter rate, root/shoot ratio(R/S), and texture properties

The dry matter content was determined following the method outlined by Yu et al. (2023). Tuberous roots, leaf, and stem samples were dried to constant mass at 80°C. The root/shoot ratio (R/S) was calculated for each of the nine samples, considering both aboveground and underground biomass, triplicate. Yield was calculated by tuberous root number per plant, fresh weight per tuberous root and planting density. Texture properties of the tuberous roots were ascertained through Textural Profile Analysis (TPA), a technique outlined by Understanding these effects could provide insights into how biochar application might be optimized to improve the yield and quality of sweet potato starch, which is a significant component of the crop's economic and nutritional value analyzed four pivotal textural attributes of tuberous roots: Hardness, Adhesiveness, Cohesiveness, and Springiness. Hardness, measured in Newtons (N), represents the maximum force encountered during the initial extrusion cycle, signifying the point at which the tuberous roots surpass its biological yield point under continuous external pressure, thereby reflecting the sample's resistance to deformation. Adhesiveness, also measured in Newtons (N), denotes the work done by the probe as it detaches from the sample surface, indicative of the root's gelling properties upon contact with the palate, teeth, and tongue during mastication. Cohesiveness is expressed as the ratio of the positive peak area during the second extrusion cycle to that of the first, mirroring the sample's resilience to fragmentation and its capacity to maintain structural integrity during chewing. Springiness is conveyed by the ratio of the heights of the second compression relative to the first, measured in millimeters (mm), which denotes the sample's ability to revert to its original form post-compression, reflecting its springiness.

2.4. Soluble sugar and starch content

Following a 130-day growth period, triplicate samples were randomly selected from each experimental pot to serve as materials for subsequent experiments. The Chinoy iodine colorimetric method quantified the starch content (Chinoy, 1939; Gur et al., 1969; McGrance et al., 1998). Meanwhile, sucrose content was evaluated through the conventional anthrone colorimetric assay. Following the manufacturer's protocols, glucose, and fructose contents were respectively determined using the glucose content detection kit (GOPOD oxidase method) and the fructose content detection kit (Resorcinol process), both provided by Ruixinbio, Quanzhou, China.

2.5. Enzymes activity of starch synthesis

The enzyme activity of starch debranching enzyme (DBE), granule-bound starch synthase (GBSS), starch branching enzyme (SBE), and soluble starch synthase (SSS) were assayed according to Nakamura et al.

(1989) and measured by the kits from Ruixinbio (Quanzhou, China). SBE activity was measured by monitoring the decrease in absorbance at 660 nm due to the reduction of the amylose-iodine complex. The reaction mixture included 65 μL of heat-inactivated enzyme solution or crude enzyme solution, 85 μL of reagent one, 10 μL of reagent two (dissolved in boiling water bath if precipitated), 130 μL of reagent three, and 10 μL of reagent four. After incubation at 37°C for 20 min and heat treatment at 95°C for 5 min, the mixture was cooled, and 200 μL was transferred to a micro-quartz cuvette or a 96-well plate for absorbance measurement at 660 nm. One unit (U) of SBE activity is defined as the amount of enzyme that causes a 1 % decrease in the absorbance of the amylose-iodine complex per milligram of protein at 37°C.SSS activity was determined using a coupled enzyme assay that measures the formation of NADPH. The reaction mixture contained 40 μL of sample, 140 μL of reagent one, 30 μL of reagent two (shaken well before use), 10 μL of reagent three, and 30 μL of reagent four. The mixture was incubated at 30°C for 20 min, followed by heat inactivation at 95–100°C for 2 min. After centrifugation at 12,000 rpm and 4°C for 10 min, the supernatant was used for the colorimetric reaction in a 96-well plate with reagents five, six, and seven. The absorbance was measured at 450 nm. One unit (U) of SSS activity is defined as the amount of enzyme catalyzing the formation of 1 nmol of NADPH per minute at 30°C.GBSS activity was assayed using a coupled enzyme assay that measures the formation of NADPH. The reaction mixture consisted of 40 μL of sample suspension, 140 μL of reagent one, 30 μL of reagent two (shaken well before use), 10 μL of reagent three, and 30 μL of reagent four. The mixture was incubated at 30°C for 20 min, followed by heat inactivation at 95–100°C for 2 min. The absorbance was measured at 450 nm. One unit (U) of GBSS activity is defined as the amount of enzyme catalyzing the formation of 1 nmol of NADPH per minute at 30°C.DBE activity was determined using a modified 3,5-dinitrosalicylic acid method. The reaction mixture contained 20 μL of sample, 200 μL of reagent two, and 280 μL of reagent three. After incubation at 37°C for 30 min, 100 μL of reagent four was added, followed by color development at 95°C for 10 min. The absorbance (ΔA) was measured at 540 nm. One unit (U) of DBE activity is defined as the amount of enzyme that releases 1.0 μmol of soluble sugars (as maltose) from branched starch per hour at 37°C.

2.6. RNA extraction and sequencing

The total RNA extraction was performed from twelve samples at four different biochar treatments by using Tiangen RNA prep Pure Plant Kit (Polysaccharides & Polyphenolics-rich) following the manufacturer's instructions (Yu et al., 2020). RNA purity and concentration were assessed on NanoDrop 2000 (Thermo Fisher Scientific, Wilmington, DE, USA), and the RNA integrity was checked using Agilent Bioanalyzer 2100 (Agilent Technologies, Palo Alto, CA, USA). The NEB Next Ultra small RNA Sample Library Prep Kit for Illumina (NEB, Ipswich, MA, USA) was used to create sequencing libraries by the manufacturer's instructions, and index codes were applied to assign sequences to specific samples. According to the manufacturer's instructions, the TruSeq PE Cluster Kit v4-cBotHS (Illumina, San Diego, CA, USA) was used to cluster the index-coded sample data on a cBot Cluster Generation System. The library preparations were sequenced and paired-end reads were generated on an Illumina HiSeqXten platform after cluster generation. The Biomarker Technologies Co., Ltd. (Beijing, China) has taken charge of mRNA isolation, fragment interruption, cDNA synthesis, adapter addition, PCR amplification, and RNA-seq. There were triplicates for each treatment.

2.7. Sequence data and differential expressed genes (DEGs) analysis

High-quality clean data (clean reads) were filtered from the raw data by removing reads containing adapters and poly-Ns as well as low-quality reads comprising more than 5 % of unknown nucleotides, which were further calculated the GC content, the Phred values, sequence duplication level. The remaining high-quality clean sequencing reads were mapped onto 'Taizhong6' database (https://www.sweetpotao.com/) using HISAT2 software (Kim et al., 2019), and then StringTie (Pertea et al., 2015) was used to assemble the above reads, and the transcriptome of which was reconstructed for subsequent analysis.

The fragments per kilobase of transcript per million fragments mapped (FPKM) as a measure of the transcript or gene expression level, were used to estimate and normalize the sweet potato gene expression levels (Li and Dewey, 2011). The DESeq2 software was used to identify differentially expressed genes (DEGs) across samples or groups (Anders and Huber, 2010). An absolute value of expression difference fold | log2FoldChange | > 1 and significance p-value< 0.05 and FDR (False Discovery Rate)<0.01 were used as thresholds to identify the DEGs (Zhou et al., 2016). The DEGs were applied to the enrichment analysis of GO functions and the KEGG pathway.

2.8. Sequence annotation and weighted gene co-expression network analysis (WGCNA)

Gene function was annotated based on the following databases by using BLAST(E value<1×10–5): Nr (the National Center for Biotechnology Information, non-redundant protein database, ftp://ftp.ncbi.nlm.nih.gov/blast/db/) COG (the Clusters of Orthologous Groups database, ftp://ftp.ncbi.nih.gov/pub/COG/COG2014/data/), Swiss-Prot database (http://web.expasy.org/docs/swiss-prot_guideline.htmL) , KOG(Clusters of orthologous groups for eukaryotic complete genomes, ftp://ftp.ncbi.nih.gov/pub/COG/KOG/kyva), Pfam (http://pfam.xfam.org/), GO (Gene Ontology, http://www.geneontology.org) and KEGG (Kyoto Encyclopedia of Genes and Genomes, http://www.genome.jp/kegg/) . To annotate the gene with Gene Ontology functional enrichment and the Kyoto Encyclopedia of Genes and Genomes (KEGG) pathway, the GOseq R package and KOBAS software were used. DEGs were significantly enriched in GO terms, and KEGG pathways were determined at p-values<0.05. Pathways analysis of upregulated and downregulated genes was performed using KEGG mapper (https://www.genome.jp/kegg/mapper.html) and Plant MetGenMAP.

2.9. qRT-PCR analysis

Total RNA from all the collected samples was extracted using SteadyPure Plant RNA Extraction Kit (AG21019, Accurate Biotechnology, Hunan, Co., Ltd.) following the manufacturer's instructions to validate the RNA-seq data. Reverse transcription was performed on 1 μg of RNA from each sample using the Evo M-MLV RT Mix Kit with gDNA Clean for qPCR (AG11728, Accurate Biotechnology, Hunan, Co., Ltd). Five representative genes from the key pathways of husk biochar were chosen for qRT-PCR analysis. qRT-PCR assay was conducted by a CFX Connect Real-Time System (Bio-Rad, USA) using SYBR Green Premix Pro Taq HS qPCR Kit (AG11701, Accurate Biotechnology, Hunan, Co., Ltd). The primer of genes for qRT-PCR detection is designed by Primer6 software listed in the supplementary Tab. S8. The sweet potato β-Actin gene (GenBank, AY905538) was applied as the internal control. The experiments were conducted for biological triplicates for each gene and the $2^{-\triangle\triangle CT}$ method was used to calculate the result (Mistry et al., 2021). Statistical significance was set to $P < 0.05$.

2.10. Statistic analysis

Statistical analysis employed one-factor analysis of variance with SPSS 23.0 (IBM, Armonk, NY, USA), and Duncan's method was utilized for mean comparisons within varieties at a significance level of $P < 0.05$. Tables were built using Excel 2021 (Microsoft Corporation, Redmond, WA, USA), and Figures were created using Excel 2021 and Adobe Illustrator 2020 software (Adobe Systems Incorporated, San Jose, CA, USA).

3. Results

3.1. Soil nutrients properties

The data on STBA's effect on soil nutrient properties is presented in Table1. The STBA increased the pH, total carbon content, nitrogen(N), and potassium(K) in the soil. It merits attention that with the escalation of biochar application concentration, there is a proportional increment in the concentrations of available nitrogen and potassium. These nutrients attain their apex levels at X20t treatment with respective values of 184.10 and 225.10. It indicated that sufficient STBA can effectively improve the nitrogen and potassium content in the soil ($P < 0.05$). Although the available phosphorus(P) of biochar(64.88±0.13) was higher than CK(37.10±0.03), the available phosphorus(P) of STBA treatments (7.85–11.66) was lower than CK.

3.2. Dry matter rate and R/S of sweet potato

As shown in Tables 2,3 the R/S and yield of all STBA treatments were higher than CK, especially X20t treatment (2132.73±30.45 g/plant) was higher than CK(1238.76±49.0 g/plant) significantly in this study ($P<0.05$). As biochar amount was increased, the yield of sweet potato was increased by 47.19–72.21 %. However, the dry matter of leaves, stems and roots of STBA treatments was not significantly different with CK.

3.3. Texture properties of tuberous root

As Table 3 shown, upon incrementing the biochar application rate, the hardness, cohesiveness, and springiness, exhibited negligible variation ($P > 0.05$). In stark contrast, adhesiveness underwent a biphasic response, initially plummeting from 10.17 N/mm in the control group (CK) to 3.50 N/mm under the 5 t·hm^{-2} biochar treatment (X5t), before a subsequent ascent. The adhesiveness of the tuberous roots after X5t and X10t application was lower than CK significantly ($P < 0.05$).

3.4. Soluble sugar and starch content

For applications such as starch extraction or serving as a resource for industrial starch, the quantity of starch in sweet potatoes is paramount (Kumar et al., 2023). As Fig. 1 shown, the starch content of sweet potato ranged from 53.45 % to 55.83 % under four different STBA treatments in this study, they are not significantly different ($P > 0.05$). The Amylose/amylopectin ratio (AM/AP) of X10t was 47.22 %, which was higher than X5t significantly in this study ($P < 0.05$). AM/AP of all STBA treatments was insignificant with CK ($P > 0.05$). Soluble sugars fulfill the crucial role of precursors in starch synthesis, offering the initial substrates necessary for this metabolic pathway (Zhai et al., 2021, Zhang et al., 2021). The sucrose, glucose, and fructose content of X5t were lower than CK and other STBA treatments significantly. However, the sucrose and glucose content of CK were the highest among all STBA treatments, with 37.41±0.83 mg/g and 72.45±1.28 mg/g, respectively. 5–10 t·hm^{-2} STBA decreased sucrose, fructose, and glucose content of tuberous root.

Table1
Soil nutrients status of the experimental soils.

Soil sample	pH	Carbon (%)	Available nitrogen (mg/kg)	Available phosphorus (mg/kg)	Available potassium (mg/kg)
Biochar	9.32 ±0.05^{a}	0.95 ±0.11^{b}	49.68 ±0.33^{b}	64.88±0.13^{a}	464.00 ±1.93^{a}
CK	6.71 ±0.03^{b}	0.71 ±0.10^{c}	2.62±0.10^{e}	37.10±0.03^{b}	50.92±0.03^{e}
X5t	6.77 ±0.01^{b}	0.76 ±0.10^{c}	28.07 ±0.21^{d}	7.85±0.15^{e}	74.74±0.05^{d}
X10t	6.81 ±0.02^{b}	1.03 ±0.26^{ab}	39.71 ±0.16^{c}	11.66±0.17^{c}	187.70 ±0.06^{c}
X20t	6.90 ±0.03^{b}	1.26 ±0.12^{a}	184.10 ±0.24^{a}	8.28±0.02^{d}	225.10 ±0.08^{b}

Note: Data are means ± SD of biological triplicates. Means denoted by the same letter do not significantly differ at $P < 0.05$, as determined by Duncan's multiple range test.

Table2
R/S, Dry matter rate, and yield of sweet potato.

Treatment	R/S	Yield (Fresh, g/plant)	Dry matter rate (%)			
			Leaf	Stem	Root (except tuberous root)	Tuberous root
CK	1.34 ±0.20^{b}	1238.76 ±49.06^{c}	19.03 ±1.02^{a}	10.05 ±1.01^{a}	28.95 ±2.55^{a}	31.18 ±2.02^{a}
X5t	1.55 ±0.23^{a}	1822.20 ±23.10^{b}	19.02 ±1.12^{a}	10.45 ±1.22^{a}	26.18 ±2.02^{a}	33.77 ±1.32^{a}
X10t	1.56 ±0.20^{a}	1881.80 ±25.18^{b}	18.43 ±1.55^{a}	9.91 ±1.04^{a}	31.47 ±3.02^{a}	31.62 ±2.55^{a}
X20t	1.57 ±0.20^{a}	2132.73 ±30.45^{a}	18.97 ±1.44^{a}	8.87 ±1.62^{a}	25.40 ±2.42^{a}	29.38 ±1.02^{a}

Note: Data are means ± SD of biological triplicates. Means denoted by the same letter do not significantly differ at $P < 0.05$, as determined by Duncan's multiple range test.

Table 3
Texture properties of tuberous root.

Treatment	Hardness N	Adhesiveness N/mm	Cohesiveness Ratio	Springiness mm
CK	106.33±8.90^{a}	10.17±3.44^{a}	0.22±0.03^{a}	5.32±0.43^{a}
X5t	110.99±9.56^{a}	3.50±2.12^{b}	0.21±0.04^{a}	4.95±0.62^{a}
X10t	109.14±9.98^{a}	4.24±2.66^{b}	0.21±0.02^{a}	4.82±0.72^{a}
X20t	107.53±8.42^{a}	6.70±3.78^{ab}	0.21±0.03^{a}	4.75±0.58^{a}

Note: Data are means ± SD of biological triplicates. Means denoted by the same letter do not significantly differ at $P < 0.05$, as determined by Duncan's multiple range test.

3.5. Enzymes activity of starch synthesis

The intricate process of starch synthesis metabolism is inextricably linked to the essential roles played by enzymes specifically associated with its production. These biological catalysts are responsible for the transformation of glucose molecules into complex carbohydrates such as starch and dextrin, highlighting their fundamental importance in carbohydrate metabolism (Zhang et al., 2021). As shown in Figs. 1, 2 and Tab. S3, the activity of the debranching enzyme (DBE) and the granule-bound starch synthase (GBSS) activity of sweet potato tuberous root under X5t STBA had the lowest activity (1.38U/g and 813.74 U/g, respectively) and significantly lower than other treatments ($P < 0.05$). For the DBE activity, the treatments were ranked as follows: X10t > X20t > CK >X5t with no significant difference between the treatment and CK ($P < 0.05$). The soluble starch synthase (SSS) activity of sweet potato tuberous root at X5t and X10t STBA was significantly lower than CK, while X20t showed similar activity to CK ($P < 0.05$). Regarding the enzymes, the treatments could be ranked, from highest SBE activity to lowest, as follows: X20t > CK > X5t> X10t, also with no significant difference between X5t and X20t ($P < 0.05$).

3.6. RNA-sequencing analysis

RNA sequencing analysis serves as a powerful tool for deciphering the complex regulatory mechanisms that crops employ to adapt their gene expression patterns in response to varying biochar environments. This approach allows researchers to peer into the genetic fine-tuning that underlies crop resilience and productivity in soils amended with

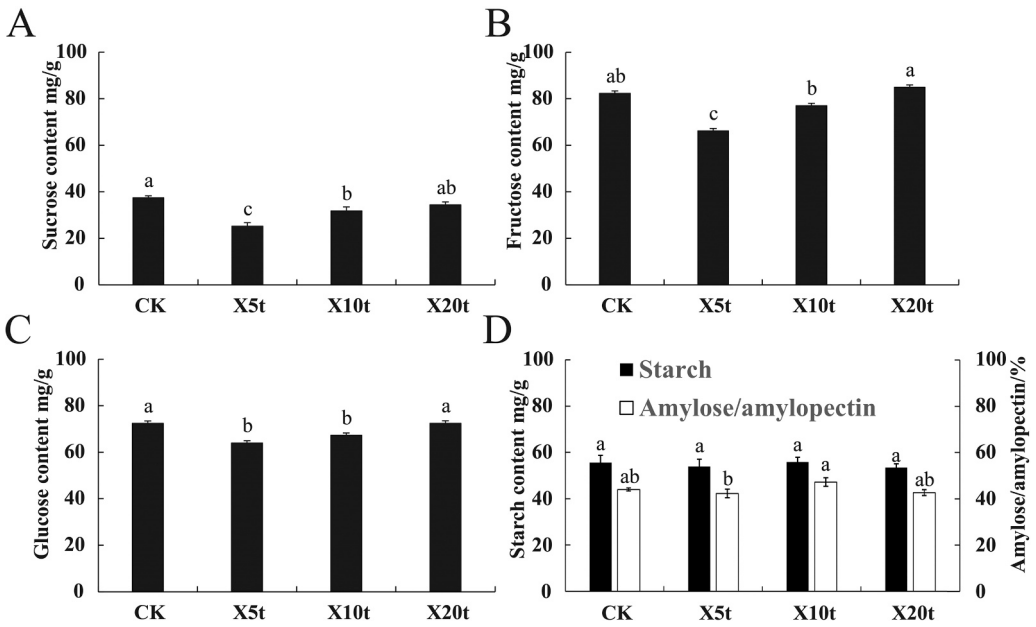

Fig. 1. Sucrose, fructose, glucose, and starch content of tuberous roots of sweet potato under STBA. (A) Sucrose content, (B) Fructose content, (C) Glucose content, (D) Starch content, and Amylose/Amylopectin ratio (AM/AP). Note: The bar plot means starch content and the red line chart means the rate of AM/AP of tuberous roots. Data are means ± SD of biological triplicates. Means denoted by the same letter do not significantly differ at $P < 0.05$, as determined by Duncan's multiple range test.

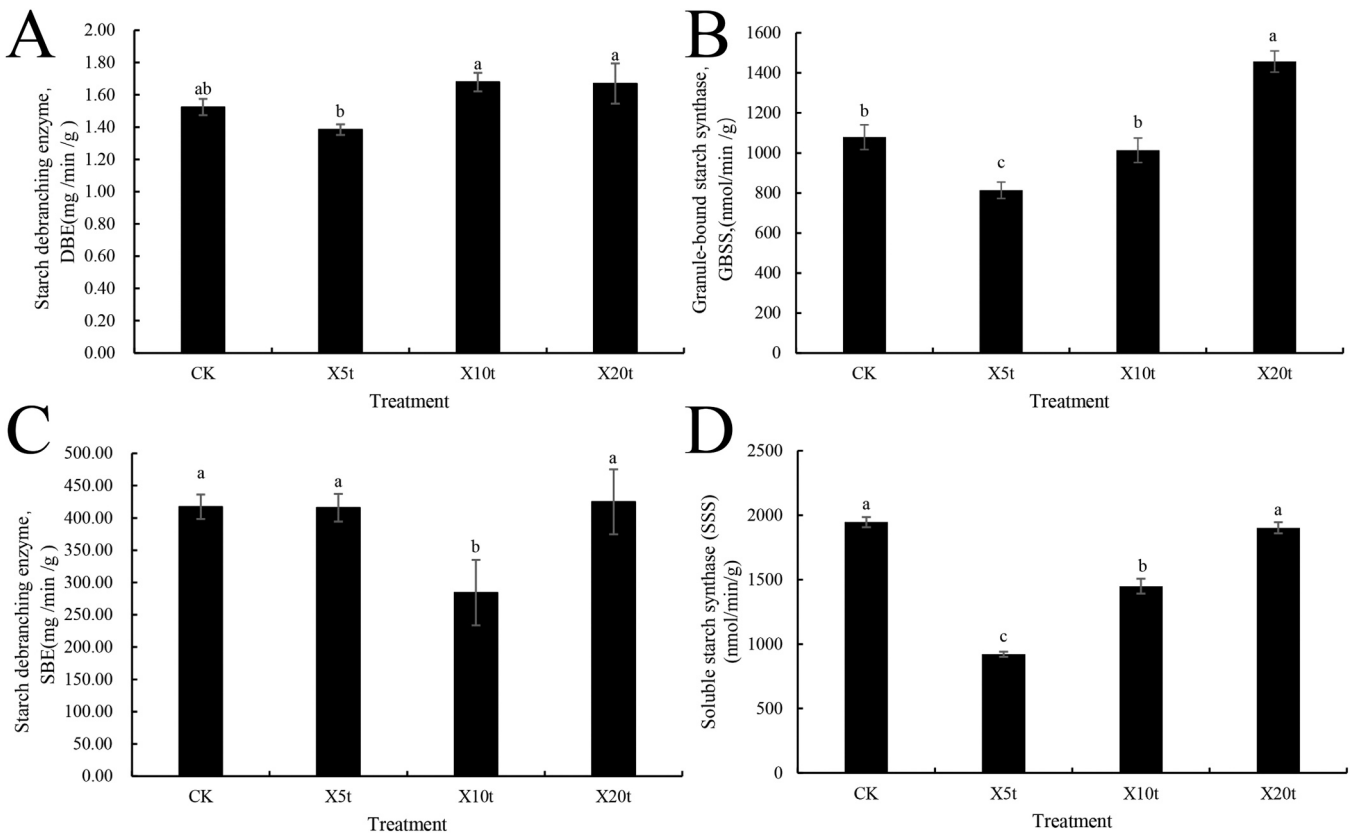

Fig. 2. Starch-related enzymes A: DBE, starch debranching enzyme; B: GBSS, granule-bound starch synthase; C: SBE, starch branching enzyme; D: SSS, soluble starch synthase.

biochar (Zhang et al., 2024). Approximately 517,237,214 clean reads and 77.40 Gb of data were generated after filtering from 12 samples of different STBA treatments. An average of 94.90 % of raw reads had a quality score of Q30 (an error probability for base calling of less than 0.1 %). A total of 432,896,245 multiple-mapped reads were obtained by comparing them to the reference genomes after removing ribosomal RNAs. The sequencing saturation curves for each sample showed that the sequencing depth met the requirements for subsequent analysis 64,

295. Overall, 64,610 genes were detected across samples, which accounted for 74.70 % of the total number of genes (74,088) in the reference group. PCA analysis and clustering of samples were performed based on gene expression level. The results of PCA analysis showed that the differences between STBA treatments and CK were more pronounced at 10 t·hm^{-2} biochar treatment (Fig. S1).

3.7. Differential gene expression (DEGs) analysis

A total of three pairwise comparative analyses (X5t_vs_CK, X10t_vs_CK, X20t_vs_CK) systematically investigated the potential molecular mechanisms of different STBA treatments (Fig. 3, Tab. S5). In total, 504 DEGs (158 up-regulated and 346 down-regulated) were detected in X5t_vs_CK, 1302 DEGs (353 up-regulated and 949 down-regulated) were detected in X10t_vs_CK, and 598 DEGs (407 up-regulated and 191 down-regulated) were detected in X20t_vs_CK (Fig. 3A). A Venn diagram illustrated the distribution of DEGs among the three comparisons (Figs. 2B, 2C). Specifically, 28 down-regulated genes and 7 up-regulated genes overlapped in X5t_vs_CK, X10t_vs_CK, X20t_vs_CK. The BLAST algorithm was utilized to annotate 6961 DEGs based on the Gene Ontology (GO), Kyoto Encyclopedia of Genes and Genomes (KEGG), Clusters of Orthologous Groups (COG), Nr, Swiss-Prot and Pfam databases to functionally characterize expression genes (Table 4). The X5t_vs_CK, X10t_vs_CK, and X20t_vs_CK comparisons exhibited 493 (97.8 %), 1287 (98.8 %), and 589 (98.50 %) DEGs, respectively.

3.8. Enrichment analysis of GO and KEGG of DEGs

GO analysis was used to classify DEGs based on their functions. The number of DEGs assigned GO terms was 401(79.56 %), 1062(81.56 %), 489(81.77 %) DEGs in the X5t_vs_CK, X10t_vs_CK and X20t_vs_CK comparisons, respectively. The GO terms included three aspects: biological process (BP), cellular component (CC), and molecular function (MF). Significant changes in BP were observed in areas such as development, reproduction, growth, and immune system functions. Large changes in MF occurred in the structural molecule, nutrition reservoir, and enzyme activity categories, while those in CC were concentrated in the cell, organelle, and macromolecular complex regions.

According to the GO enrichment analysis, it was worth noting that exposure to biochar greatly influenced the BP, CC, and MF(Fig. 4). The most common biological process GO term among the DEGs was the 'response to stimulus', which had the largest number of genes detected in the three comparisons. Notably, three cellular components GO terms were significantly enriched in the comparisons of X5t_vs_CK and X10t_vs_CK, such as 'intrinsic component of plasma membrane', 'apoplast', and 'plasma membrane part', while no cellular component was detected in the X20t_vs_CK comparison.

We conducted a KEGG pathway analysis to identify active biological processes in the selected STBA treatments. In this analysis, we identified 14, 36, and 14 enriched functional categories in the X5t_vs_CK, X10t_vs_CK, and X20t_vs_CK, comparisons, respectively. Additionally, 1, 16, and 8 significantly enriched functional categories($P<0.05$) were identified for the DEGs in the three comparisons, respectively. Under the 5 t·hm^{-2} STBA (Fig. 5A), 504 DEGs were analyzed for KEGG enrichment. map09101 (Carbohydrate metabolism), was significantly enriched ($P<0.05$). For the 10 t·hm^{-2} STBA treatment, 1302 DEGs were employed for KEGG enrichment analysis. Sixteen representative pathways were significantly enriched. including map00194 (Photosynthesis proteins), map00195(Photosynthesis), map00196 (Photosynthesis - antenna proteins), map09101 (Carbohydrate metabolism), map02000 (Transporters), map00860 (Porphyrin and chlorophyll metabolism), map00500 (Starch and sucrose metabolism) and map00400 (Phenylalanine, tyrosine and tryptophan biosynthesis).

We employed 598 DEGs from the X20t_vs_CK for KEGG enrichment analysis (Fig. 5C). Eight representative pathways were significantly enriched, including map04075 (Plant hormone signal transduction), map09132(Signal transduction), map00860 (Porphyrin and chlorophyll metabolism). Additionally, map00500 (Starch and sucrose metabolism), and map09101 (Carbohydrate metabolism) were enriched under all biochar applications, which indicated that with an increase in biochar application, certain representative pathways also become more prominent. Sweet potatoes exhibited significant biological changes in carbon metabolism, nitrogen metabolism, photosynthesis, sucrose metabolism, and amino acid metabolism among other pathways. It is noteworthy that protein and amino acid metabolism were significantly altered by biochar application.

3.9. Expression of genes involved in metabolic pathways of sucrose and starch metabolic pathways

In this study, there are 48 DEGs involved in starch and sucrose metabolism showed special expression patterns (Fig. 6, Tab. S6). Specifically, under 5t·t·hm^{-2} biochar treatment compared to CK, three DEGs were upregulated, 10 DEGs were downregulated. Similarly, under 10 t·t·hm^{-2} biochar treatment, four DEGs were upregulated, and 21 DEGs were downregulated compared to CK. 11 DEGs were upregulated, and 5 DEGs were downregulated compared to CK in X20t biochar

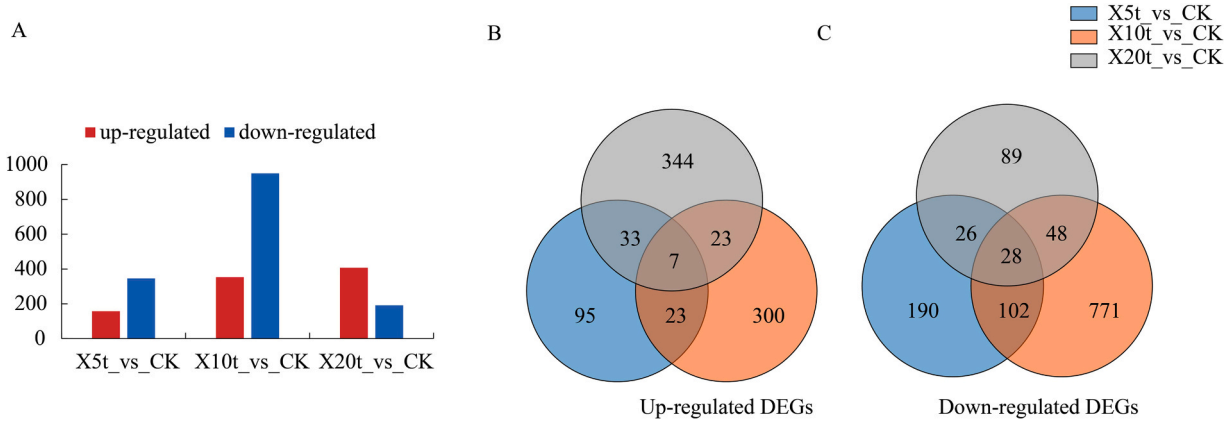

Fig. 3. DEGs between different STBA treatments. (A) Numbers of DEGs in X5t_vs_CK, X10t_vs_CK, X20t_vs_CK. the x-axis shows the paired samples; the y-axis shows the number of DEGs; the red bars represent significantly up-regulated genes($P< 0.05$); the blue bars represent significantly down-regulated genes($P< 0.05$). (B) Venn diagrams of up-regulated DEGs numbers and distributions among three comparisons. (C) Venn diagrams of down-regulated DEGs numbers and distributions among three comparisons. The blue circles represent the number of DEGs in X5t_vs_CK; The yellow circles represent the number of DEGs in X10t_vs_CK; the gray circles represent the number of DEGs in X20t_vs_CK.

Table4
Annotation summaries of DEGs.

DEG set	Annotated DEGs	GO	KEGG	COG	Nr	Swiss-Prot	Pfam
X5t_vs_CK	493	401	195	464	492	420	442
X10t_vs_CK	1287	1062	610	1234	1284	1141	1185
X20t_vs_CK	589	489	231	555	587	496	532

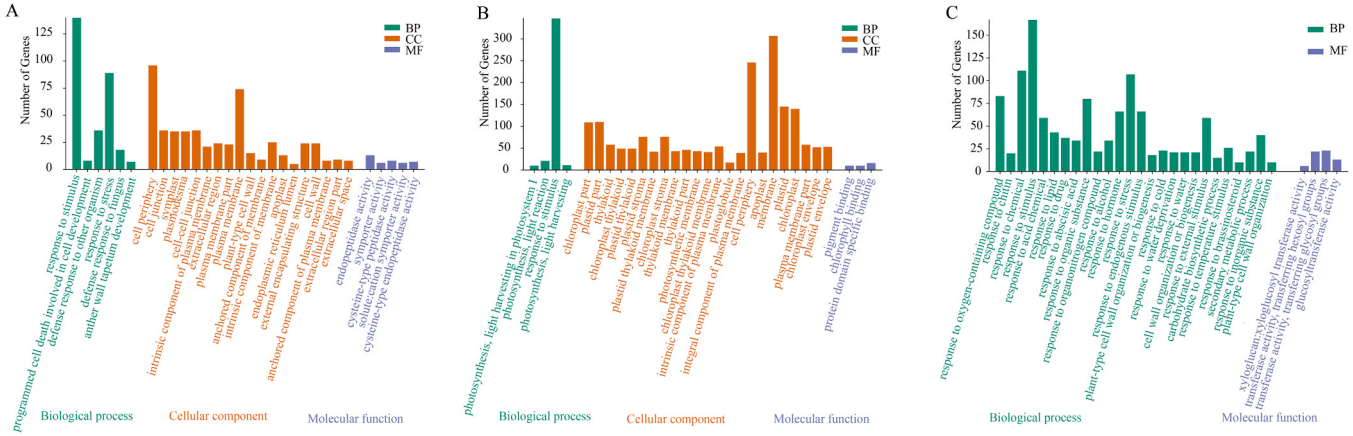

Fig. 4. The enrichment analysis of the DEGs using GO enrichment. (A–C) GO classifications of DEGs in X5t_vs_CK, X10t_vs_CK and X20t_vs_CK, respectively. The y-axis indicates the number of DEGs, and the X-axis indicates the top 30 enriched GO terms. The green-orange and purple colors represent biological processes, cellular components and molecular function, respectively.

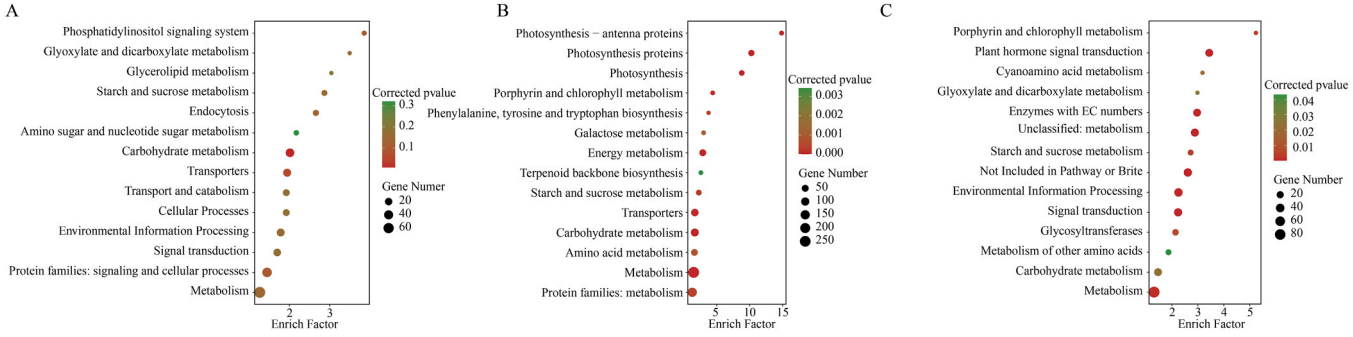

Fig. 5. KEGG pathway enrichment of DEGs under different STBA treatments. A) KEGG enrichment map of DEGs in X5t_vs_CK; B) KEGG enrichment map of DEGs in X10t_vs_CK; C) KEGG enrichment map of DEGs in X20t_vs_CK.

treatment. Sucrose synthesis and hydrolysis are catalyzed by Sucrose Phosphate Synthase (SPS) and Sucrose Synthase (SuSy). SuSy primarily catalyzed sucrose hydrolysis rather than its synthesis (Li et al., 2014). SuSy decomposes sucrose into UDP-glucose and fructose, providing substrates for starch synthesis, and can also convert UDP-glucose and fructose back into sucrose (Zhai et al., 2021). We detected a total of 13 *SuSy* genes with diverse expression patterns, showing low expression across all treatments. Among these, nine *SuSy* genes included two up-regulated genes (*g49561*, *g55056*) and seven down-regulated genes (*g20167, g30039, g505, g55342, g60893, g9231, g9241*) in X10t and four DEGs (3 up-regulated (*g57705, g9225, g9227*) and one down-regulated (*g20130*)) in X20t, while no DEGs were detected in X5t biochar treatment.

It was obvious that no DEGs were involved in the starch synthesis pathway. indicating a consistent pattern in starch conversion to sugars during tuberous root development in sweet potatoes. Starch degradation primarily occurs via the phosphorolytic pathway, catalyzed by the phosphorylase and amylolytic enzymes. Key enzymes such as β-glucosidase(bglX), α-amylase (AMY), and β-amylase (BMY) play crucial roles in starch and sucrose metabolism. In this study, two *IbAMY* genes (*g59290*, *g59297*), one *IbbglB* gene (*g46466*), and one *IbbglX* (*g51057*) were down-regulated in X5t_vs_CK, while the gene(*g13691*) encoding *IbBMY*, along with two genes (*g59316*, *g31641*) encoding *IbbglB* were down-regulated in X10t_vs_CK. In X20t_vs_CK, three genes (*g24112*, *g24863*, *g4495*) encoding *IbbglX*, *g59316* encoding *IbbglB* and *g38231* encoding *IbBMY* were up-regulated while *g13691* encoding *IbBMY* and *g51057*(*bglX*) were down-regulated.

Sucrose degradation into trehalose is facilitated by trehalose 6-phosphate phosphatase (*otsB*) and trehalose-phosphate synthase (*TPS*). However, compared to CK, *g16754* encoding *IbotsB* was down-regulated under X5t and X10t treatment but up-regulated under X20t biochar treatment. The starch was converted into dextrin under the regulation of *g38321*, *g13691*, *g59290,* and *g59297*. The synthesis and metabolism of cellobiose and D-glucose were mediated by β-glucosidase (*IbbglX*, *IbbglB*) and endoglucanase (*IbGN*). RNA-seq data revealed that *IbbglX* and *IbbglB* showed down-regulation in X5t and X10t but showed up-regulation (*g24112, g24863, g4495, g59316*) in X20t biochar treatment.

Note: INV, invertase; GN, glucan endo^{-1},3-β-glucosidase; SuSy, sucrose synthase; SPS, sucrose-phosphate synthase; bglX, β-glucosidase; bglB, β-glucosidase; malZ, α-glucosidase; EG, endoglucanase; AMY, α-amylase; BMY, β- amylase; TPS, trehalose 6-phosphate synthase; otsB, trehalose 6-phosphate phosphatase; TREH, α-trehalase

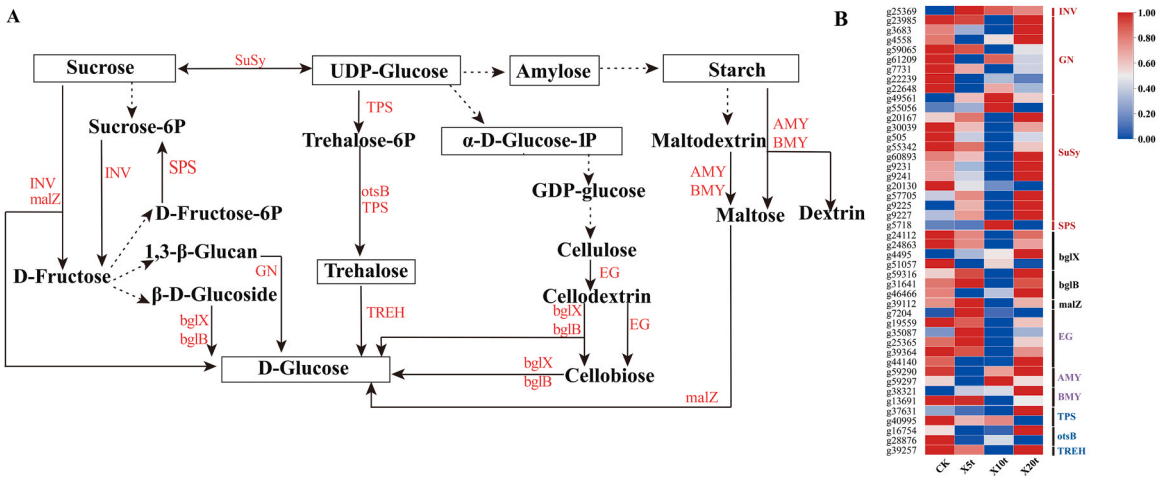

Fig. 6. Starch and sucrose metabolism pathway and expression pattern heatmap of related genes. A) Hypothetical representation of the expression patterns of DEGs involved in the starch and sucrose metabolism in tuberous roots. Upregulated Genes were shown in red, downregulated genes in blue, and non-DEGs in white. B) Expression pattern of related genes in starch and sucrose metabolism pathway.

3.10. Classified the DEGs by WGCNA

Due to the extensive number of samples analyzed by using transcriptome sequencing, we classified the DEGs by WGCNA (Fig. 7A). All genes were classified into eight modules with a particular focus on the magenta module based on its gene expression pattern. Overall, with the increase of biochar application, the expression of the magenta module exhibited higher levels in the X5t, X10t, and X20t compared to the control group. KEGG enrichment of the DEGs within this module revealed significant enrichment in the processes related to plant hormone signal transduction (Fig. 7B). By mapping the genes involved in plant hormone signal transduction, we found that the application of biochar altered the regulation of abscisic acid, auxin, and brassinosteroid (Fig. S3, Tab. S7).

3.11. qRT-PCR validation of the expression of selected genes

We selected five genes that showed substantial change in the RNA-data, including *g26948*(*IAA*) and *g13864* (*SAUR*) for plant hormone signal transduction and two genes namely *α-amylase* gene(*AMY*, *g59297*), *β-amylase* gene (*BMY*, *g13691*) and glucan endo^{-1},3-β-glucosidase (*GN*, *g61209*) in starch and sucrose metabolism verified by qRT-PCR. Specifically, *g26948* and *g13691* displayed down-regulation while *g13864* was up-regulated under 5 t·hm^{-2} and 10 t·hm^{-2} biochar application. Additionally, *g59297* showed down-regulated under 5 t·hm^{-2} biochar application. We observed that the changes in gene expression between different biochar treatments matched the RNA-seq results. However, the fold changes differed, possibly indicating differences in sensitivity between the two methods. The consistent results obtained from the qRT-PCR and RNA-seq analyses suggested that the RNA-seq data were reproducible and reliable (Fig. 8).

4. Discussion

Biochar can enrich soil nutrients and enhance soil particle structure, thereby fostering a more conducive environment for plant growth (Edussuriya et al., 2023). The nutritional profile of biochar is contingent upon the source materials used in its preparation. Biochar derived from fecal matter and sludge tends to be replete with phosphorus, whereas that derived from plant materials is often abundant in potassium (Hossain et al., 2020). Sweet potato has higher K requirements, and K plays key roles in the growth and the economic yield (Wang et al., 2017; Adekiya et al., 2022). In the present study, biochar treatment resulted in a significantly higher available K content in the soil (74.74(X5t)-225.10 mg/kg(X20t)) and higher yield, which indicated that available K exhibited significant positive correlation with yield and improve soil K

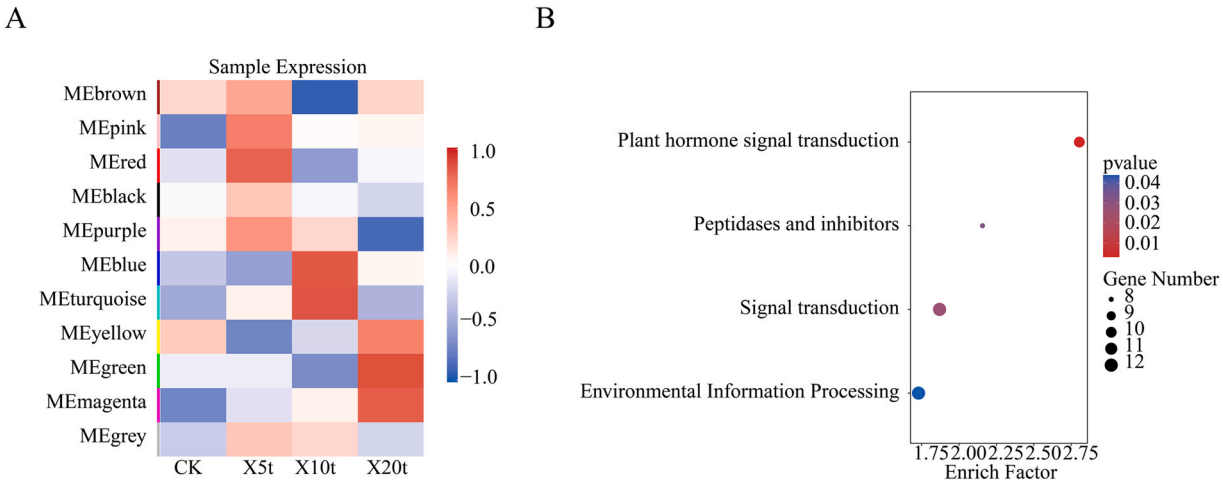

Fig. 7. Functional analysis of key expression patterns of WGCNA. A) Expression patterns of different modules of WGCNA; B) KO enrichment bubble diagram of genes in the magenta module;.

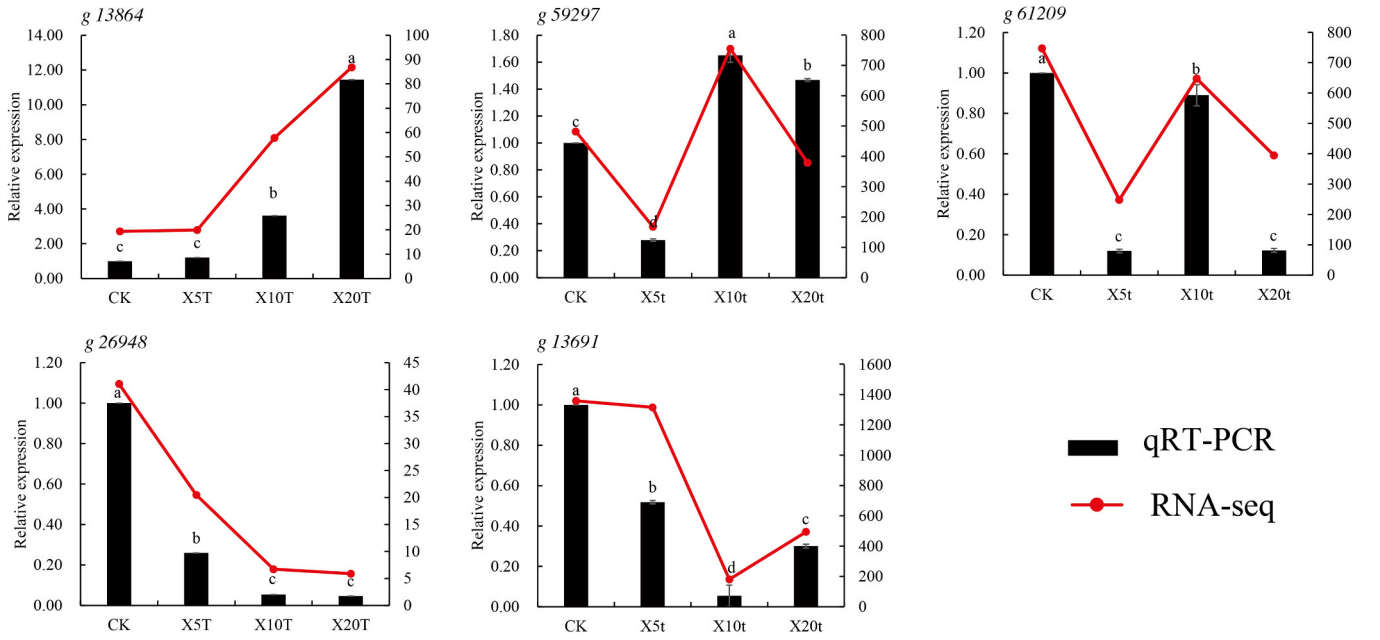

Fig. 8. qRT-PCR validation of representative genes in key pathways affected by biochar application.

availability. Additionally, the soil's pH value increased after biochar application might due to the alkaline nature of biochar. Although biochar is rich in available phosphorus and promotes the efficiency of phosphorus application (Luo et al., 2023), the available phosphorus content of the treatments' soil was lower than that of the control group (CK), indicating that the quantity of biochar ($\geq$5 t·hm^{-2}) applied could potentially sequester available phosphorus within the soil matrix, consequently diminishing its bioavailability to plants. In acid soils, elevated levels of reactive iron and aluminum can react with phosphates to form insoluble compounds, thereby diminishing the phosphorus uptake by plants (Bouray et al., 2021). Previous studies found that the application of biochar significantly reduces the available phosphorus in the rice rhizosphere at long-term (4–9 years) (Yuan et al., 2024; Chen et al., 2022; Jiang et al., 2021). In this study, first-year found this phenomenon. Therefore, to address the potential reduction in phosphorus availability due to increased soil pH from biochar application, it is suggested that future soil management practices include the incorporation of phosphorus fertilizers or the modification of biochar properties. These proactive measures are intended to optimize phosphorus accessibility, ensuring that plants can more effectively absorb this vital nutrient for their growth and development (Luo et al., 2023).

Starch is the main component of sweet potato tuberous roots. It determines the yield of sweet potatoes (Guo et al., 2019). Previous studies have reported that the nitrogen (N) level of soil can influence the growth and development of sweet potato as well as the correlation of starch content and physical properties. Recently, the properties of starches from sweet potato Jishu 25 with the application of N fertilizer (0, 75, and 150 kg/ha), concluded that the level of N treatment affects the amylose content and pasting properties of starch, but shows little effect on starch size and thermal properties (Duan et al., 2019).However, Noda et al. (1996) reported that the level of fertilizer cannot affect the physicochemical properties of starch in two purple- and two yellow-fleshed sweet potato varieties. In this study, compared with CK, biochar treatments resulted in a significantly higher available N content in the soil which increased by 10.70(X5t) to 70.26 times(X20t), but showed a significantly lower starch content(53.43 mg/g) and amylose content (34.71 mg/kg) in X20t. These results might due to the reason that the high N fertilization decreases the amylose content of starch. Li et al. (2013) reported that the high N fertilization treatment decreases the amylose of wheat. Zhu et al. (2017) observed that the application of high nitrogen levels enhances the swelling and gelatinization properties of rice starch, while concurrently reducing its granule size, amylose content, gelatinization temperature, and pasting viscosity.

In this study, we found the available nitrogen and potassium content of the soil increased in STBA treatments. However, the texture properties and starch quality of sweet potatoes were not significantly different from CK, although the enzyme of starch synthesis of sweet potato changed significantly after STBA. A potential explanation for this observation is that STBA upregulates the expression of SPS and SuSy, which in turn stimulates the synthesis of precursors required for starch production. It has a greater effect on starch accumulation than SSS, DBE, etc. This observation is consistent with prior findings in soybeans, where short-term biochar application (STBA) was found to elevate the activity of SPS and SuSy, thereby influencing carbohydrate metabolism. (Zhu et al., 2019). Furthermore, sweet potatoes may exhibit growth-stage-specific responses to biochar, which could dynamically adjust over time. The plants might counteract the synthetic effects of biochar on starch by fine-tuning the rate of starch degradation, thereby maintaining a relatively stable starch content. It is well-known that sucrose converts into glucose and fructose catalyzed by INV. UDP-glucose, synthesized from sucrose degradation catalyzed by sucrose synthase SuSy, served as a substrate for trehalose-6P synthesis mediated by trehalose-6-phosphate synthase (TPS, EC 2.4.1.15). Additionally, we also identified several transcripts encoding pivotal enzymes involved in sucrose and starch metabolic pathways, including sucrose degradation, synthesis pathways, starch degradation, and trehalose degradation pathways. (Chen et al., 2018) Trehalose-6P represents an initial product in trehalose biosynthesis, which is for plant signal metabolic pathways (Li et al., 2014; Paul et al., 2008). Furthermore, studies in *Arabidopsis thaliana*, showed that the sucrose induction would elevate the TPS substrates and UDP-glucose, suggesting that sucrose might activate TPS, ultimately promoting an increase in trehalose-6P levels (Li et al., 2014). KEGG pathway analysis revealed a potential new sucrose hydrolysis pathway in sweet potato tuberous roots under biochar treatment (Fig. 6), implying that sucrose might convert into trehalose-6P through *SuSy* and *TPS*, subsequently converting into trehalose by trehalose 6-phosphate phosphatase (otsB and TPS, EC: 3.1.3.12). We further validated gene expression related to sucrose and starch metabolism in different biochar treatments using qRT-PCR analyses, confirming the expression of DEGs. In summary, biochar application positively

influenced sucrose degradation through its impact on sucrose and starch metabolic pathways.

Plant hormones like gibberellic acid (GA), auxin (IAA), abscisic acid (ABA), cytokinin (CTK), and jasmonic acid, play major roles in root development and growth regulation (Wang and Irving, 2011). CTK and ABA are specifically involved in the formation of stored roots (Matsuo et al., 1983, 1988; Nakatani and Komeichi, 1991). WGCNA analysis showed that the plant hormone signal transduction pathway was enriched in tuberous roots under different biochar treatments. Auxin, essential for cambium cell multiplication and proliferation (Noh et al., 2010), also maintains cambium cells in a meristem state and enhances xylem component quality. The expression of auxin-related genes AUX/IAA and SAUR, were dramatically up-regulated during the tuberous root expansion stage of the *Raphanus sativus*, *Rehmannia glutinosa,* and *Callerya speciosa* (Li et al., 2015; Yu et al., 2016; Yao et al., 2021)., suggesting their role in cell expansion during secondary growth of cambium. ABA plays a role in tuberous root thickening by stimulating meristem cell division (Cai et al., 2022). Two distinct ABA signal transduction pathways have been identified: the PYLs-PP2C-SnRK2 pathway (Liu et al., 2022) and the CHLH-WRAKY pathway, which have been demonstrated to play a role in the regulation of fruit ripening (Sun et al., 2011; Chai et al., 2011; Jia et al., 2011). Additionally, ABA plays a role in tuberous root thickening by stimulating meristem cell division (Cai et al., 2022). Previous research has linked PP2C to plant abiotic stress tolerance (Saez et al., 2004; Lu et al., 2019; Zhang et al., 2017), while ABA has been associated with the sugar response pathway (Rook et al., 2006). Low sucrose levels induced *AtSUC9*, increasing ABA levels through ABA-inducible genes, and enhancing resilience to abiotic stress (Jia et al., 2015). In our study, *g26948* encoding PP2C showed down-regulated under X10t and X20t biochar applications. These findings suggest that biochar application may influence in plant tolerance to abiotic stress. In summary, the application of biochar exerts a complex influence on the tuberous roots of sweet potatoes, affecting both starch and sucrose metabolic processes, as well as plant hormone signaling pathways. These impacts collectively lead to enhancements in yield and the sweet potatoes' resilience against environmental stressors.

5. Conclusions

This study demonstrates that STBA substantially increased sweet potato yields and enhanced soil fertility, with optimal effects of 20 $t \cdot hm^{-2}$ STBA. While the adhesiveness and soluble sugar of tuberous root decreased at 5–10 $t \cdot hm^{-2}$ STBA, it had no significant impact on starch content or the AM/AP ratio. STBA enhances sweet potato yields without compromising starch quality, crucial for producing industrial-grade sweet potatoes. Biochar likely augments sweet potato yields and stress tolerance by modulating key enzymatic activities and plant hormone signaling, such as SPS, SuSy, IAA, and ABA. STBA effectively increases the yield of sweet potatoes without negatively affecting their quality, confirming its status as a potent strategy for yield enhancement in sweet potato cultivation. Consequently, STBA not only boosts the yields and stress tolerance of sweet potatoes but also maintains the integrity of their starch, establishing a solid scientific foundation for the application of biochar in agricultural practices.

CRediT authorship contribution statement

Ximing Xu: Writing – review & editing, Writing – original draft, Visualization, Resources, Project administration, Methodology, Investigation, Funding acquisition, Data curation, Conceptualization. **Jingzhen Zhang:** Writing – original draft, Visualization. **Zunfu Lv:** Resources, Project administration, Funding acquisition. **Taojun Li:** Formal analysis, Data curation. **Jing Li:** Funding acquisition. **Yueming Zhu:** Validation. **Guoquan Lu:** Software, Funding acquisition.

Declaration of Competing Interest

Authors declared that they have no conflicts of interest to this work. We declare that we do not have any commercial or associative interest that represents a conflict of interest in connection with the work submitted.

Acknowledgements

This research was funded by Research funding project of Zhejiang Provincial Department of Education (Y202147184), Scientific Research Foundation for the Introduction of Talent by Zhejiang A&F University (2021LFR017), China Agriculture Research System (CARS-10), the Natural Science Foundation of China (32071897, 32272222, and 32372075), the Key Research and Development Program of Zhejiang Province (2021C02057), and Huzhou Public Welfare Application Research Key Project (2023GZ47).

Appendix A. Supporting information

Supplementary data associated with this article can be found in the online version at doi:10.1016/j.indcrop.2024.120050.

Data availability

Data will be made available on request.

References

Abideen, Z., Koyro, H.W., Huchzermeyer, B., Ansari, R., Zulfiqar, F., Gul, B., 2020. Ameliorating effects of biochar on photosynthetic efficiency and antioxidant defence of Phragmites karka under drought stress. Plant Biol. 22, 259–266.

Adekiya, A.O., Adebiyi, O.V., Ibaba, A.L., Aremu, C., Ajibade, R.O., 2022. Effects of wood biochar and potassium fertilizer on soil properties, growth and yield of sweet potato (Ipomoea batatas). Heliyon 8, e11728.

Agbede, T.M., Oyewumi, A., Agbede, G.K., Adekiya, A.O., Adebiyi, O.T.V., Abisuwa, T. A., Ijigbade, J.O., Ogundipe, C.T., Wewe, A.O., Olawoye, O.D., Eifediyi, E.K., 2024. Impacts of poultry manure and biochar amendments on the nutrients in sweet potato leaves and the minerals in the storage roots. Sci. Rep. 14, 16598.

Alengebawy, A., Ran, Y., Ghimire, N., Osman, A.I., Ai, P., 2023. Rice straw for energy and value-added products in China: a review. Environ. Chem. Lett. 1–32.

Anders, S., Huber, W., 2010. Differential expression analysis for sequence count data. Genome Biol. 11, R106.

Bouray, M., Moir, J.L., Lehto, N.J., Condron, L.M., Touhami, D., Hummel, C., 2021. Soil pH effects on phosphorus mobilization in the rhizosphere of *Lupinus angustifolius*. Plant Soil 469, 387–407.

Cai, Z., Cai, Z., Huang, J., Wang, A., Ntambiyukuri, A., Chen, B., Zheng, G., Li, H., Huang, Y., Zhan, J., Xiao, D., He, L., 2022. Transcriptomic analysis of tuberous root in two sweet potato varieties reveals the important genes and regulatory pathways in tuberous root development. BMC Genom. 23, 473.

Chai, Y.M., Jia, H.F., Li, C.L., Dong, Q.H., Shen, Y.Y., 2011. *FaPYR1* is involved in strawberry fruit ripening. J. Exp. Bot. 62, 5079–5089.

Chen, H., Yuan, J., Chen, G., Zhao, X., Wang, S., Wang, D., Wang, L., Wang, Y., Wang, Y., 2022. Long-term biochar addition significantly decreases rice rhizosphere available phosphorus and its release risk to the environment. Biochar 4, 54.

Chen, L., Sun, P., Zhou, F., Li, Y., Chen, K., Jia, H., Yan, M., Gong, D., Ouyang, P., 2018. Synthesis of rebaudioside D, using glycosyltransferase UGTSL2 and in situ UDP-glucose regeneration. Food Chem. 259, 286–291.

Chen, S., Zhang, X., Shao, L., Sun, H., Niu, J., Liu, X., 2020. Effects of straw and manure management on soil and crop performance in North China Plain. CATENA 187, 104359.

Chinoy, J.J., 1939. A new colorimetric method for the determination of starch applied to soluble starch, natural starches, and flour. *Mikrochemie vereinigt.* Mit. Mikrochim. Acta 26, 132–142.

Duan, W.X., Zhang, H.Y., Xie, B.T., Wang, B.Q., Zhang, L.M., 2019. Impacts of nitrogen fertilization rate on the root yield, starch yield and starch physicochemical properties of the sweet potato cultivar Jishu 25. PLoS One 14, e0221351.

Edussuriya, R., Rajapaksha, A.U., Jayasinghe, C., Pathirana, C., Vithanage, M., 2023. Influence of biochar on growth performances, yield of root and tuber crops and controlling plant-parasitic nematodes. Biochar 5, 68.

Gabhane, J.W., Bhange, V.P., Patil, P.D., Bankar, S.T., Kumar, S., 2020. Recent trends in biochar production methods and its application as a soil health conditioner: a review. SN Appl. Sci. 2, 1307.

Gong, D.K., Xu, X.M., Wu, L.A., Dai, G.J., Zheng, W.J., Xu, Z.J., 2020. Effect of biochar on rice starch properties and starch-related gene expression and enzyme activities. Sci. Rep. 10, 16917.

Gong, W., Yan, X., Wang, J., Hu, T., Gong, Y., 2009. Long-term manure and fertilizer effects on soil organic matter fractions and microbes under a wheat–maize cropping system in northern China. Geoderma 149, 318–324.
Guo, K., Liu, T., Xu, A., Zhang, L., Bian, X., Wei, C., 2019. Structural and functional properties of starches from root tubers of white, yellow, and purple sweet potatoes. Food Hydrocoll. 89, 829–836.
Gur, A., Cohen, A., Bravdo, B.-A., 1969. Colorimetric method for starch determination. J. Agric. Food Chem. 17, 347–351.
Haider, F.U., Wang, X., Farooq, M., Hussain, S., Cheema, S.A., Ain, N.U., Virk, A.L., Ejaz, M., Janyshova, U., Liqun, C., 2022. Biochar application for the remediation of trace metals in contaminated soils: implications for stress tolerance and crop production. Ecotoxicol. Environ. Saf. 230, 113165.
Hossain, M.Z., Bahar, M.M., Sarkar, B., Donne, S.W., Ok, Y.S., Palansooriya, K.N., Kirkham, M.B., Chowdhury, S., Bolan, N., 2020. Biochar and its importance on nutrient dynamics in soil and plant. Biochar 2, 379–420.
Jia, H.F., Chai, Y.M., Li, C.L., Lu, D., Luo, J.J., Qin, L., Shen, Y.Y., 2011. Abscisic acid plays an important role in the regulation of strawberry fruit ripening. Plant Physiol. 157, 188–199.
Jia, W., Zhang, L., Wu, D., Liu, S., Gong, X., Cui, Z., Cui, N., Cao, H., Rao, L., Wang, C., 2015. Sucrose transporter AtSUC9 mediated by a low sucrose level is involved in Arabidopsis abiotic stress resistance by regulating sucrose distribution and aba accumulation. Plant Cell Physiol. 56, 1574–1587.
Jiang, B., Shen, J., Sun, M., Hu, Y., Jiang, W., Wang, J., Li, Y., Wu, J., 2021. Soil phosphorus availability and rice phosphorus uptake in paddy fields under various agronomic practices. Pedosphere 31, 103–115.
Kim, D., Paggi, J.M., Park, C., Bennett, C., Salzberg, S.L., 2019. Graph-based genome alignment and genotyping with HISAT2 and HISAT-genotype. Nat. Biotechnol. 37, 907–915.
Kumar, Y., Shikha, D., Guzmán-Ortiz, F.A., Sharanagat, V.S., Kumar, K., Saxena, D.C., 2023. Starch: current production and consumption trends. Starch: Advances in Modifications, Technologies and Applications. Springer International Publishing, Cham, pp. 1–10.
Lai, Y.C., Wang, S.Y., Gao, H.Y., Nguyen, K.M., Nguyen, C.H., Shih, M.C., Lin, K.H., 2016. Physicochemical properties of starches and expression and activity of starch biosynthesis-related genes in sweet potatoes. Food Chem. 199, 556–564.
Li, B., Dewey, C.N., 2011. RSEM: accurate transcript quantification from RNA-Seq data with or without a reference genome. BMC Bioinform. 12, 323.
Li, M., Yang, Y., Li, X., Gu, L., Wang, F., Feng, F., Tian, Y., Wang, F., Wang, X., Lin, W., Chen, X., Zhang, Z., 2015. Analysis of integrated multiple 'omics' datasets reveals the mechanisms of initiation and determination in the formation of tuberous roots in Rehmannia glutinosa. J. Exp. Bot. 66, 5837–5851.
Li, W.H., Shan, Y.L., Xiao, X.L., Zheng, J.M., Luo, Q.G., Ouyang, S.H., Zhang, G.Q., 2013. Effect of nitrogen and sulfur fertilization on accumulation characteristics and physicochemical properties of a- and b-wheat starch. J. Agric. Food Chem. 61, 2418–2425.
Li, X., Wang, C., Cheng, J., Zhang, J., Da Silva, J.A., Liu, X., Duan, X., Li, T., Sun, H., 2014. Transcriptome analysis of carbohydrate metabolism during bulblet formation and development in *Lilium davidii* var. unicolor. BMC Plant Biol. 14, 358.
Liu, S., Lu, C., Jiang, G., Zhou, R., Chang, Y., Wang, S., Wang, D., Niu, J., Wang, Z., 2022. Comprehensive functional analysis of the PYL-PP2C-SnRK2s family in *Bletilla striata* reveals that BsPP2C22 and BsPP2C38 interact with BsPYLs and BsSnRK2s in response to multiple abiotic stresses. Front. Plant Sci. 13, 963069.
Lu, T., Zhang, G., Wang, Y., He, S., Sun, L., Hao, F., 2019. Genome-wide characterization and expression analysis of PP2CA family members in response to ABA and osmotic stress in Gossypium. PeerJ 7, e7105.
Luo, D., Wang, L., Nan, H., Cao, Y., Wang, H., Kumar, T.V., Wang, C., 2023. Phosphorus adsorption by functionalized biochar: a review. Environ. Chem. Lett. 21, 497–524.
Lyu, R., Ahmed, S., Fan, W., Yang, J., Wu, X., Zhou, W., Zhang, P., Yuan, L., Wang, H., 2021. Engineering properties of sweet potato starch for industrial applications by biotechnological techniques including genome editing. Int. J. Mol. Sci. 22, 9533.
Matsuo, T., Mitsuzono, H., Okada, R., Itoo, S., 1988. Variations in the levels of major free cytokinins and free abscisic acid during tuber development of sweet potato. J. Plant Growth Regul. 7, 249–258.
Matsuo, T., Yoneda, T., Itoo, S., 1983. Identification of free cytokinins and the changes in endogenous levels during tuber development of sweet potato (*Ipomoea batatas* Lam.). Plant Cell Physiol. 24, 1305–1312.
McGrance, S.J., Cornell, H.J., Rix, C.J., 1998. A Simple and Rapid Colorimetric Method for the Determination of Amylose in Starch Products. Starch - Stärke 50, 158–163.
Mistry, J., Chuguransky, S., Williams, L., Qureshi, M., Salazar, G.A., Sonnhammer, E.L.L., Tosatto, S.C.E., Paladin, L., Raj, S., Richardson, L.J., Finn, R.D., Bateman, A., 2021. Pfam: the protein families database in 2021. Nucleic Acids Res. 49, D412–D419.
Nakamura, Y., Yuki, K., Park, S.-Y., Ohya, T., 1989. Carbohydrate metabolism in the developing endosperm of rice grains. Plant Cell Physiol. 30, 833–839.
Nakatani, M., Komeichi, M., 1991. Changes in the endogenous level of zeatin riboside, abscisic acid and indole acetic acid during formation and thickening of tuberous roots in sweet potato. Jpn J. Crop Sci. 60, 91–100.
Noda, T., Takahata, Y., Sato, T., Ikoma, H., Mochida, H., 1996. Physiochemical properties of starches from purple and orange fleshed sweet potato roots at two levels of fertilizer. Starch 48, 395–399.
Noh, S.A., Lee, H.S., Huh, E.J., Huh, G.H., Paek, K.H., Shin, J.S., Bae, J.M., 2010. SRD1 is involved in the auxin-mediated initial thickening growth of storage root by enhancing proliferation of metaxylem and cambium cells in sweetpotato (Ipomoea batatas). J. Exp. Bot. 61, 1337–1349.
Paul, M.J., Primavesi, L.F., Jhurreea, D., Zhang, Y., 2008. Trehalose metabolism and signaling. Annu Rev. Plant Biol. 59, 417–441.
Pertea, M., Pertea, G.M., Antonescu, C.M., Chang, T.C., Mendell, J.T., Salzberg, S.L., 2015. StringTie enables improved reconstruction of a transcriptome from RNA-seq reads. Nat. Biotechnol. 33, 290–295.
Rook, F., Hadingham, S., Li, Y., Bevan, M., 2006. Sugar and ABA response pathways and the control of gene expression. Plant, Cell Environ. 29, 426–434.
Saez, A., Apostolova, N., Gonzalez-Guzman, M., Gonzalez-Garcia, M.P., Nicolas, C., Lorenzo, O., Rodriguez, P.L., 2004. Gain-of-function and loss-of-function phenotypes of the protein phosphatase 2C HAB1 reveal its role as a negative regulator of abscisic acid signalling. Plant J. 37, 354–369.
Sayara, T., Basheer-Salimia, R., Hawamde, F., Sánchez, A., 2020. Recycling of organic wastes through composting: process performance and compost application in agriculture. Agronomy 10, 1838.
Singh, H., Northup, B.K., Rice, C.W., Prasad, P.V.V., 2022. Biochar applications influence soil physical and chemical properties, microbial diversity, and crop productivity: a meta-analysis. Biochar 4, 8.
Singh Yadav, S.P., Bhandari, S., Bhatta, D., Poudel, A., Bhattarai, S., Yadav, P., Ghimire, N., Paudel, P., Paudel, P., Shrestha, J., Oli, B., 2023. Biochar application: a sustainable approach to improve soil health. J. Agric. Food Res. 11, 100498.
Sun, L., Wang, Y.P., Chen, P., Ren, J., Ji, K., Li, Q., Li, P., Dai, S.J., Leng, P., 2011. Transcriptional regulation of SlPYL, SlPP2C, and SlSnRK2 gene families encoding ABA signal core components during tomato fruit development and drought stress. J. Exp. Bot. 62, 5659–5669.
Tao, J., Wan, C., Leng, J., Dai, S., Wu, Y., Lei, X., Wang, J., Yang, Q., Wang, P., Gao, J., 2023. Effects of biochar coupled with chemical and organic fertilizer application on physicochemical properties and in vitro digestibility of common buckwheat (Fagopyrum esculentum Moench) starch. Int. J. Biol. Macromol. 246, 125591.
Tisserant, A., Cherubini, F., 2019. Potentials, limitations, co-benefits, and trade-offs of biochar applications to soils for climate change mitigation. Land 8, 179.
Walter, R., Rao, B.K.R., 2015. Biochars influence sweet-potato yield and nutrient uptake in tropical Papua New Guinea. J. Plant Nutr. Soil Sci. 178, 393–400.
Wang, J.D., Hou, P., Zhu, G.P., Dong, Y., Hui, Z., Ma, H., Xu, X.J., Nin, Y., Ai, Y., Zhang, Y., 2017. Potassium partitioning and redistribution as a function of K-use efficiency under K deficiency in sweet potato (*Ipomoea batatas* L.). Field Crops Res. 211, 147–154.
Wang, Y.H., Irving, H.R., 2011. Developing a model of plant hormone interactions. Plant Signal. Behav. 6, 494–500.
Yao, S., Lan, Z., Huang, R., Tan, Y., Huang, D., Gu, J., Pan, C., 2021. Hormonal and transcriptional analyses provides new insights into the molecular mechanisms underlying root thickening and isoflavonoid biosynthesis in Callerya speciosa (Champ. ex Benth.) Schot. Sci. Rep. 11, 9.
Ye, X., Abe, S., Zhang, S., 2020. Estimation and mapping of nitrogen content in apple trees at leaf and canopy levels using hyperspectral imaging. Precis. Agric. 21, 198–225.
Yu, J.J., Su, D., Yang, D.J., Dong, T.T., Tang, Z.H., Li, H.M., Han, Y.H., Li, Z.Y., Zhang, B. H., 2020. Chilling and heat stress-induced physiological changes and microrna-related mechanism in sweetpotato (*Ipomoea batatas* L.). Front. Plant Sci. 11, 687.
Yu, R., Wang, J., Xu, L., Wang, Y., Wang, R., Zhu, X., Sun, X., Luo, X., Xie, Y., Everlyne, M., Liu, L., 2016. Transcriptome profiling of taproot reveals complex regulatory networks during taproot thickening in radish (*Raphanus sativus* L.). Front. Plant Sci. 7, 1210.
Yu, Y., Kleuter, M., Dinani, S.T., Trindade, L.M., Van Der Goot, A.J., 2023. The role of plant age and leaf position on protein extraction and phenolic compounds removal from tomato (*Solanum lycopersicum*) leaves using food-grade solvents. Food Chem. 406, 135072.
Yuan, J., Chen, H., Chen, G., Pokharel, P., Chang, S.X., Wang, Y., Wang, D., Yan, X., Wang, S., Wang, Y., 2024. Long-term biochar application influences phosphorus and associated iron and sulfur transformations in the rhizosphere. Carbon Res. 3, 25.
Zhai, Z.Y., Keereetaweep, J., Liu, H., Xu, C.C., Shanklin, J., 2021. The role of sugar signaling in regulating plant fatty acid synthesis. Front. Plant Sci. 12, 643843.
Zhang, K., Wu, Z., Tang, D., Luo, K., Lu, H., Liu, Y., Dong, J., Wang, X., Lv, C., Wang, J., Lu, K., 2017. Comparative transcriptome analysis reveals critical function of sucrose metabolism related-enzymes in starch accumulation in the storage root of sweet potato. Front. Plant Sci. 8, 914.
Zhang, M., Mukhamed, B., Yang, Q., Luo, Y., Tian, L., Yuan, Y., Huang, Y., Feng, B., 2023. Biochar and nitrogen fertilizer change the quality of waxy and non-waxy broomcorn millet (*Panicum miliaceum* L.) starch. Foods 12, 3009.
Zhang, X., Feng, X., Chai, N., Kuzyakov, Y., Zhang, F., Li, F.-M., 2024. Biochar effects on crop yield variability. Field Crops Res. 316, 109518.
Zhang, X., Guo, D., Blennow, A., Zörb, C., 2021. Mineral nutrients and crop starch quality. Trends Food Sci. Technol. 114, 148–157.
Zhou, Q., Guo, J.-J., He, C.-T., Shen, C., Huang, Y.-Y., Chen, J.-X., Guo, J.-H., Yuan, J.-G., Yang, Z.-Y., 2016. Comparative transcriptome analysis between low- and high-cadmium-accumulating genotypes of pakchoi (Brassica chinensis L.) in response to cadmium stress. Environ. Sci. Technol. 50, 6485–6494.
Zhu, D., Zhang, H., Guo, B., Xu, K., Dai, Q., Wei, C., Zhou, G., Huo, Z., 2017. Effects of nitrogen level on structure and physicochemical properties of rice starch. Food Hydrocoll. 63, 525–532.
Zhu, Q., Kong, L.J., Shan, Y.Z., Yao, X.D., Zhang, H.J., Xie, F.T., Ao, X., 2019. Effect of biochar on grain yield and leaf photosynthetic physiology of soybean cultivars with different phosphorus efficiencies. J. Integr. Agric. 18, 2242–2254.